

April 2014

In Flight Recharging of MAVs

George P. Abbiati
Worcester Polytechnic Institute

John Paul Croteau
Worcester Polytechnic Institute

Timothy Kevin Grupp
Worcester Polytechnic Institute

Follow this and additional works at: <https://digitalcommons.wpi.edu/mqp-all>

Repository Citation

Abbiati, G. P., Croteau, J. P., & Grupp, T. K. (2014). *In Flight Recharging of MAVs*. Retrieved from <https://digitalcommons.wpi.edu/mqp-all/2049>

This Unrestricted is brought to you for free and open access by the Major Qualifying Projects at Digital WPI. It has been accepted for inclusion in Major Qualifying Projects (All Years) by an authorized administrator of Digital WPI. For more information, please contact digitalwpi@wpi.edu.

IN FLIGHT RECHARGING OF MICRO AERIAL VEHICLES

Major Qualifying Project Report completed in partial fulfillment

Of the Bachelor of Science degree at

Worcester Polytechnic Institute, Worcester, MA

Submitted to:

Professor Isa Bar-On

Professor Andrew Trapp

George Abbiati

John Croteau

Timothy Grupp

1 May 2014

Table of Contents

Table of Figures	3
Table of Tables	3
Acknowledgments.....	4
Abstract.....	5
Introduction	6
Background	8
Energy Regeneration Systems in Use by Aircraft Today	8
Unexplored Methods	9
The Transmitter.....	10
The Receiver.....	10
Methods.....	12
Analysis of Model Airplane	12
Analysis of Inertia Recovery System	13
Analysis of energy transmission method.....	16
Results.....	19
Energy Consumption of Aircraft	19
Regenerative braking	19
Data Limitations	22

Laser method	24
Application to aircraft	26
Conclusion.....	29
Bibliography	30
Appendix 1: Wind Tunnel Testing Data	32
Appendix 2: Descent Profiles for Different Constant Descent Angles.....	35
Appendix 3: Average Data from Laser Tests	38

Table of Figures

Figure 1: Flight Path Utilizing Regenerative Braking and Updraft	10
Figure 2: Power return as a function of wind speed.....	20
Figure 3: Energy rate (power) return	21
Figure 4: Energy return	21
Figure 5: Velocity profile of optimum slope	22
Figure 6: Plot of results of laser experiment.....	24
Figure 7: Solar Cell Efficiency	25
Figure 8: Method 1, Variable Magnification Lens on Ground	27
Figure 9: Method 2, Constant Magnification Lens on Aircraft	28

Table of Tables

Table 1: Regenerative Braking Results.....	20
--	----

Acknowledgments

Our team would like to thank the following individuals for the time and effort they gave to help our project succeed. Without them, this project would not have been possible.

- Professor Bar-On and Professor Trapp who challenged us to push ourselves and to explore outside of our engineering comfort zone. Additionally, for the extended time to mentor us through this entire year and project.
- Professor Emanuel for helping us to further understand the electrical systems needed to fulfill the requirements of our experiments and the analysis of these systems.
- Professor Furlong who shared his knowledge of lasers and optics, and took the time to train us and let us use his laser equipment.
- Professor Olinger for teaching us to use the wind tunnel and for allowing us to use them for our project.
- Morteza Meybodi Khaleghi for his help, advice, and willingness to assist us with our laser experiment.
- Worcester Polytechnic Institute and the Mechanical Engineering Department for making this project a reality.

Abstract

The flight duration of Micro Aerial Vehicles (MAVs) is frequently limited to one hour or less; an improved flight time is desired. Our project focuses on two methods of recharging MAV batteries in flight: treating the MAV propeller as a wind turbine to regenerate energy during descent and the transmission of energy to the MAV from a ground source via laser. In order to determine feasibility, we constructed proof of concepts for these options.

Introduction

Micro aerial vehicles (MAVs) are a popular surveillance tool used by the US military as well as intelligence and environmental agencies. AeroVironment produces the world's most widely used unmanned aerial system, the Raven (AeroVironment Raven, 2013). The Raven is an electrically powered vehicle that can be piloted remotely or programmed to autonomously follow a route using an onboard GPS system. It is armed with an infrared camera and features the below specifications:

RQ-11B Raven	
Flight time	60 min
Speed	32-81 km/h
Wing span	1.4 m
Mass	1.9 kg
Battery type	Lithium polymer

Small payload capacities of MAVs restrain the battery size which consequently limits flight duration. Our MQP focuses on methods of recharging batteries during flight in order to overcome shortcomings in battery capacity. Some recharge methods, such as the solar technology, have already been explored on MAVs. We investigated two means of recharging batteries in-flight which have not been significantly applied to MAVs; they are inertial recovery and the wireless transmission of energy.

The inertial recovery system trades the potential energy of altitude for potential energy stored within the MAV's battery. This is accomplished by first gaining altitude by utilizing updrafts in thermals. During the resulting descent, power is generated when the propeller spins the motor- similar to a wind turbine. During our project, we determined the maximum return rate of the inertia recovery system. In the energy transmission method, a laser (transmitter) transmits energy to a photovoltaic cell (receiver), commonly called solar cell, on the MAV recharging the battery. We explored how much energy could be

transferred by a laser to a solar cell to determine the feasibility of the laser system. In order to measure the success of each method, we compared the increase in flight duration due to the energy return against the time spent deviating from the flight path to recharge the batteries.

Background

Energy Regeneration Systems in Use by Aircraft Today

Sail planes were the first aircraft to use regenerative technology. By flying through upward air currents, sail planes increase their altitude and potential energy as seen in the below equation (Scott, 2005):

$$\text{Potential Energy} = \text{mass} \times \text{gravity} \times \text{differential in height}$$

A sail plane stores energy exclusively by virtue of position while other airplanes primarily store energy in batteries or fuel tanks. In updrafts, sail planes climb at approximately 300 feet/minute and can reach altitudes as high as 35,000 feet (Scott, 2005; Soarfl, 2013). While sail planes are typically manned aircraft, an unpiloted aircraft demonstrated the capability to autonomously locate and fly in updrafts in 2008 (Edwards & Silverberg, 2010). The aircraft completed a flight of over 5 hours by utilizing updrafts and achieved this without input from human operators. This demonstrates that unpiloted aircraft have the ability to locate and fly in updrafts. However, we did not find an example of a MAV utilizing updrafts.

Solar technology is another form of energy regeneration used in some airplanes such as the Solar Impulse HB-SIA. The HB-SIA is powered by four electric motors, has a wingspan of 71 feet, and features 11,628 mono-crystalline silicon solar cells which give the aircraft a flight duration of over 26 hours (Solar Impulse HB-SIA Datasheet, 2013). While solar technology is applicable to large aircraft, it could not produce enough power to offset the added weight of the panels on small MAVs (AeroVironment News & Events, 2013). This changed in August 2013 when cutting edge solar panels made of gallium arsenide were placed on AeroVironment's largest MAV, the Puma. It features a wingspan of 9.2 feet, more than twice as long as AeroVironment's other MAVs (AeroVironment Puma

Data Sheet, 2013). The solar panels were manufactured by Alta Devices and increased the flight endurance of the Puma system by over 350% in a test flight (AeroVironment News & Events, 2013).

Solar technology has drawbacks. The advanced surveillance capabilities in MAVs allow them to function at night (AeroVironment Raven, 2013). However, solar panels lose functionality in low light conditions. For this reason, we explored other options of recharging during flight to increase flight duration under any conditions.

Unexplored Methods

We investigated two methods of recharging MAV batteries in flight. The first is regenerative braking which is becoming common in land vehicles but has not been applied to aircraft. The second method is the wireless transmission of energy to the MAV from the ground.

In cars without regenerative braking, the brake pads convert the kinetic energy of movement into heat during deceleration. This energy leaves the system (vehicle) and enters the environment. Regenerative braking captures some of the kinetic energy normally lost to the environment, which improves efficiency (Turpen, 2013). Some electric vehicles convert the energy of velocity into potential energy using the vehicle's electric motors. When driving, the vehicle's batteries create a current driving the motors and creating torque. During deceleration, this process is reversed. The wheels apply a torque to the motors inducing a current and charging the vehicle's battery. During our MQP, we considered the propeller equivalent to the wheel and the braking phase similar to the dive portion of flight. This could be coupled with the sail plane strategy of increasing altitude via thermals and then diving to increase battery levels. As far as we are aware, no research on this concept has been published.

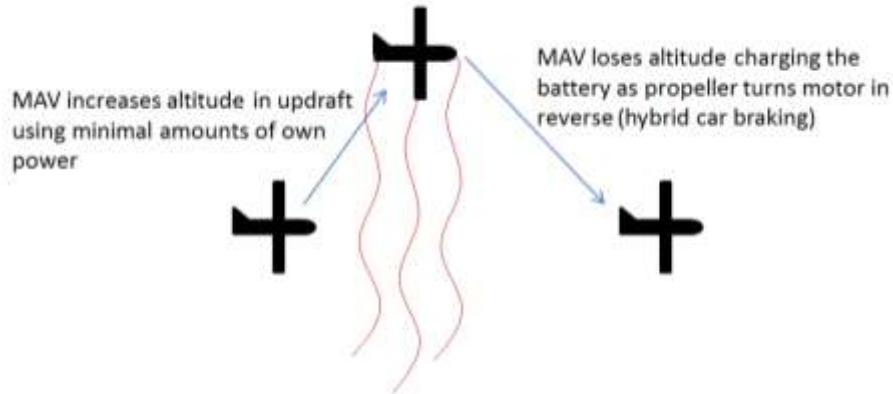


Figure 1: Flight Path Utilizing Regenerative Braking and Updraft

The second method we investigated was transferring energy during flight from a ground source to the MAV. This requires a transmitter (on the ground) and receiver (on the MAV). We explored a laser transmitter and photovoltaic cell receiver.

The Transmitter

“Laser” stands for light amplification by stimulated emission of radiation. At the core of a laser is a crystal, gas, or glass that emits photons when its electrons are energized (NASA: Lasers). The photons exit forming laser light waves. The process begins when a flash lamp pulse bombards the laser core with electrons dropping the energy level of core electrons and emitting a photon. A system of mirrors directs the emitted photon back through the core initiating the emission of more photons. This process is called amplification.

The Receiver

Solar cells transfer light energy to electrical energy. The first practical application of solar cells was in the space industry during the 1960s (Knier, 2002). A decade later, the technology migrated to earth bound applications. Solar cells are made of a semiconductor material such as silicon (San Jose State University, 2014). Electrons within the semiconductor occupy either the valence band or the

conduction band (Sukhatme & Nayak, 2008). The valence band is at a lower energy level and is fully occupied with electrons. The conduction band is at a higher energy level and is not fully occupied with electrons. The band gap energy is defined as the difference between the minimum energy of electrons in the conduction band and the maximum energy level of electrons in the valence band. Electrons jump from the valence band to the conduction band when photons from a light source (commonly the sun) with greater energy than the band gap are absorbed into the solar cell. This creates empty space in the valence band which allows for electron flow. Solar cells are doped to have N-type and p-type layers. Doping is achieved by adding impurities with a different number of electrons than the semi-conductor creating an electrically imbalanced material. The n-type layer is doped so that it has extra electrons while the p-type is doped to have extra electron holes. Electrons from the n-type layer flow to the p-type layer creating an electron potential gradient. The electron potential gradient drives the flow of electrons that the previously discussed light photons have freed. Today, silicon solar cells are the most commonly used solar cells. The most advanced silicon solar cells have an energy conversion efficiency of 25.6%, which was achieved by Panasonic in 2014 (Davis, 2014).

Lasers have already transferred energy to solar cells (Kawashima & Takeda, 2008). In tests, a small powered kite airplane was able to maintain an altitude of 50 meters while energized by a 200 watt laser. The laser was focused on the gallium arsenide cells attached to the kite plane. The resulting output power of the laser onto the solar cells was 42 watts; a laser to solar cell transfer efficiency of 21%. The benefits of the laser system include compact size of both transmitter and receiver. With the laser method, a line of sight from the laser to the aircraft must be maintained during charging. During the powered kite experiment, the laser over-heated the photovoltaic cell while attempting to transfer large amounts of energy. This was likely because the laser shone directly on the solar cell without being expanded to strike a large enough area. The energy was concentrated over to small of an area for the solar cell to withstand.

Methods

The goal of our project is investigate proof of concepts and to determine the feasibility of inertial recovery and laser transmission methods of increasing the flight duration of MAVs. To achieve our goal, we developed the following methodology, which includes analysis of the model airplane, analysis of the inertial recovery system, and analysis of the energy transmission system. The following sections explain how we achieved each objective and detail each method's purpose.

Analysis of Model Airplane

Since the power consumption data of MAVs is not published, we substituted a remote control (RC) airplane as our model. All of our testing was done on this platform. The RC aircraft is a similar size and weight as MAVs and we assumed that the power consumption is on the same order of magnitude.

First we conducted an analysis of the RC model airplane:

1. Analyze the aerodynamic components of the model RC plane and propeller.
2. Determine the power consumption of the RC plane.

We needed to calculate the drag and lift of our RC plane during flight to enable us to accurately determine our flight path and velocity profile of the descent in Matlab. We calculated drag and lift using the following two equations:

$$Drag = C_D * \left(\frac{\rho * V^2}{2} \right) * A_D$$

$$Lift = C_L * \left(\frac{\rho * V^2}{2} \right) * A_L$$

In the drag equation, C_D stands for drag coefficient, ρ is the density of the air, V is the velocity, and A_D is the total frontal area of the aircraft. We determined the drag coefficient by calculating the theoretical drag of a streamline body and the theoretical drag of a wing. In the lift equation, our lift

coefficient (C_L) was determined by researching actual data gathered from real-world aircraft of similar size. The lift coefficient depends on many factors so we selected the lowest C_L of any aircraft with a similar size as our RC model. This is the worst-case lift capability and is the poorest performance we could obtain from the airframe.

We determined the power consumption of our RC plane using the plane's battery specifications and flight duration. The below equation allowed us to determine the total energy consumed over the entire flight duration:

$$\text{Total energy consumed} = \text{battery storage capacity (mA s)} \times \text{voltage} \times \text{depth of discharge}$$

The battery storage capacity and voltage rating was published in the RC plane's user manual. Depth of discharge is the percentage of battery capacity that the battery discharges and was found through research. We knew the total flight duration of our RC plane from experience flying the aircraft. By dividing the total energy consumed by the flight duration, we calculated the average power consumption during flight. We later compared this power consumption to the energy production rate of both energy return systems to determine the overall feasibility of each method. For example, if our systems recharge at a rate of 2 Watts and the airframe consumes 2 Watts, it would be inconvenient to use the system because the same amount of time must be spent recharging the aircraft as spent on mission. As the recharge rate increases, the time spent recovering energy decreases while the time spent on mission increases.

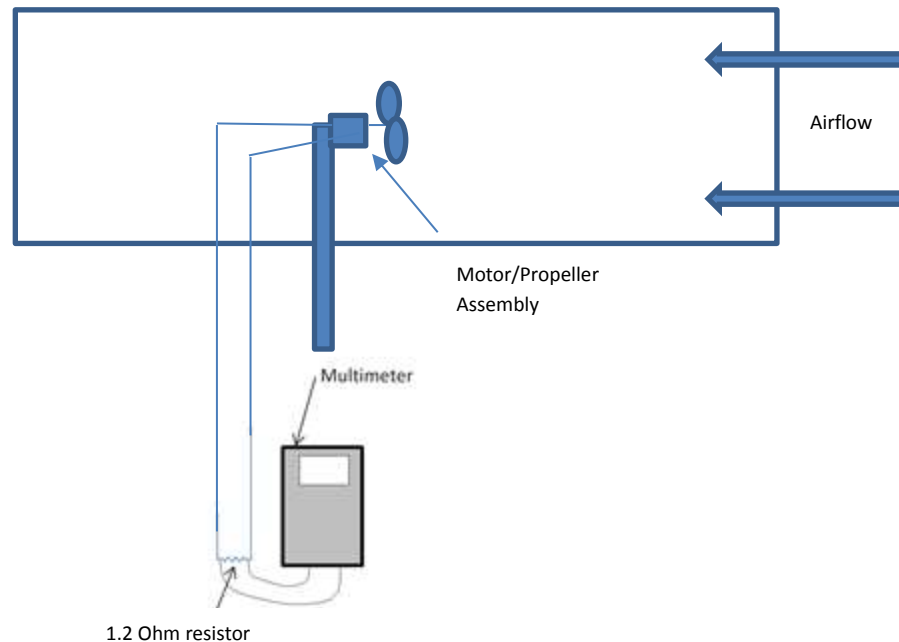
Analysis of Inertia Recovery System

After analyzing the RC aircraft, we analyzed the feasibility of an inertia recovery system on the RC model aircraft. This was done using the objectives determined below:

1. Determine the relationship between airspeed across the propeller and recharge rate.
2. Calculate the maximum recharge rate.

3. Compare the maximum recharge rate of the inertia recovery system to consumption rate and determine feasibility.
4. Determine the descent flight path, velocity profile, and time of descent of our RC plane given a descent angle.

To calculate the amount of power produced by our RC aircraft's propeller and motor at different speeds, we used a wind tunnel to simulate airflow across the propeller. The motor assembly was removed from the model RC aircraft and attached to a post and placed in the middle of the wind tunnel test area (see figure below).



The wire leads coming from the motor were then attached to a simple circuit which consisted of a 1.2 ohm resistor. We chose this value because it mimics the resistance of a four-cell nickel cadmium battery (an appropriate size and type of battery for RC airplanes) during recharging. The wind tunnel was then started at our maximum speed of 25 m/s and lowered incrementally by approximately .5 m/s until the propeller stopped spinning at the minimum spin speed of the propeller/motor combination. At each .5 m/s increment, the motor was attached to the resistor and the voltage across the resistor measured. The equation $P = \frac{V^2}{R}$ was used to determine power produced by the motor as R was known

(1.2 ohms) and the V was measured. The test was run three separate times and the resulting average data gave us our power function. Appendix 1 details the results.

In order to complete our 4th objective in this section and determine the amount of energy recovered during descent, a Matlab script was created. The script modeled in 2D what would happen to a falling aircraft by using the ODE 45 solver. We came up with realistic numbers for the lift, drag, and weight of the aircraft. Once this was completed, those numbers were input into the equations of motion so that the script took them into account. This would ensure that special aerodynamic properties such as terminal velocity were modeled correctly. We then ensured we could control essential initial conditions such as height, speed, descent angle, etc. Additionally, the script was written so that velocity, angle relative to the horizon, and flight trajectory were computed and plotted on three different graphs so we could clearly identify trends and data. In our script, the initial altitude, initial velocity, and descent angle were variables we could change. We held initial velocity to zero and selected an initial height of 480 m. This represents an aircraft exiting a thermal with zero velocity from an altitude 480 m. We realize that an aircraft would have a small exit velocity but opted to use a zero initial velocity because it represents the case that would produce the smallest energy return.

We ran the script for descent angles ranging from -5 to -85 degrees (decreasing every 5 degrees) and examined the resulting descent and velocity plots for each descent angle. Those descent paths with a terminal velocity that did not exceed the minimum spin speed of our propeller/motor combination were discarded because they would not produce any power.

Using Matlab we calculated the best fit equations for the velocity profiles as a function of time for descent angles that produced a velocity that exceeded the minimum spin speed of our propeller/motor combination. We then took our descent equations and substituted them as variable into our power equation and integrated over the total flight time. An example of this is shown below:

$$\text{Velocity Profile Equation} = 3t^2 + 4t + 2$$

$$\text{Power Return Equation} = 16v^3 + 13.5v^2 + 5v + 20$$

$$\text{Total Energy Return For Descent Angle} = \int_0^t 16\alpha^3 + 13.5\alpha^2 + 5\alpha + 20 \, dt$$

where $\alpha = 3t^2 + 4t + 2$ and t =the total descent time.

This gave us a total energy return in joules which we then divided by the total flight time to give us the average power return rate in Watts. Once this was completed, we compared return rates for all of the descent angles to determine which angle provided the greatest energy return.

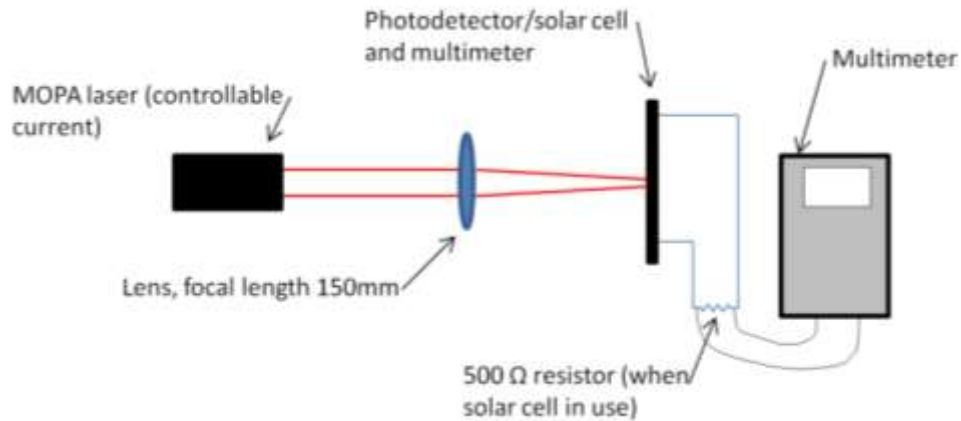
Analysis of energy transmission method

We developed the following objectives for our laser transmission method:

1. Determine the maximum amount of energy per area that can be transmitted in a simple system of laser transmitter to photovoltaic receiver without an additional cooling mechanism.
2. Compare return rate per solar cell area to power consumption and determine the required solar cell area and laser characteristics.

Our RC plane consumes 20 W of power. Because of this consumption rate and because solar cell conversion efficiency is approximately 20%, a powerful laser is required to transfer enough energy to create sustainable flight. Such a laser is very expensive and not available to us. We elected to focus on a scaled down version of the energy transfer as a proof of concept.

To conduct our laser experiment we used a laser, focal lens, photo detector, solar cell, resistor and multimeter as shown in the graphic below:



For the first part of our experiment, the laser beam passed through the focusing lens and onto a photo detector placed at the focal point. The focusing lens had a 150 mm focal length and focused the laser beam to an elliptical dot with a major diameter of .0855 mm and a minor diameter of .0810 mm. We ran the laser at low power and incrementally increased it. Through this method an equation was generated for laser output power as a function of current entering the laser. We then replaced the photo detector with a solar cell, and ran the laser with a low powered beam and incrementally increased the power. For each power level, the beam was allowed to shine on the solar cell for 20 seconds, which created a current in the solar cell that passed through a 500 Ω resistor. The voltage drop across the resistor was determined using a multimeter at the end of the 20 second period. We used the following equation to determine the power generated by the solar cell in this experiment:

$$P = \frac{V^2}{R}$$

After shining the laser on the solar cell for 20 seconds, we took the temperature at the surface of the solar cell using an IR thermometer. Once this was completed, the laser was turned off and the solar cell was allowed to return to room temperature before the next power level was tested. In order to calculate our solar cell efficiency, we tested our solar cell during mid-day in Connecticut. This was used to help provide a baseline to compare our data. Since our elliptical laser dot size remained

constant, we divided the power produced by the dot surface area to yield the power produced per area of solar cell struck by the laser.

The first step in determining the overall feasibility was to calculate the amount of energy we could transfer per solar cell area without damaging the solar cell. For example, assume our results showed that the highest possible energy produced per solar cell area was 40 W/m^2 when bombarded by a laser. Our RC plane, which consumes 20 W during flight, would need a minimum of 0.5 m^2 of solar cells exposed to a laser to transfer enough energy to produce sustainable flight. Given the size of MAVs, this is too large of an area and the laser transfer method would not be feasible.

Results

Energy Consumption of Aircraft

We calculated the energy consumption rate of our RC plane according to the equations in our methods. The RC plane battery produces 8.4 volts and has storage of 3600 Amp-seconds. We assumed a battery depth of discharge of 95% which corresponds to a Nickel Cadmium battery that has been through 500 cycles (Tech Bulletin, 1994). From experience flying the RC plane, we know that the flight duration varies from 20-25 minutes. For our calculations we used the average and assumed a flight duration 22.5 minutes. This produced an average consumption rate during the flight duration of 20.2 W.

Regenerative braking

When we placed the propeller and motor from our model RC airplane in a wind tunnel, we observed that the power generated by the motor increased as the wind speed increased. Thus, the faster the aircraft descends, the higher the power return rate. The figure below shows that our peak power produced was nearly 8.7 W and occurred at our highest airspeed, 25 m/s. The minimum power produced was .1W which occurred at a wind speed of 11 m/s. At speeds below 11 m/s, the propeller failed to spin and did not produce power. The data shown below is an average of three different trials in the wind tunnel. Using excel, a best-fit function was determined.

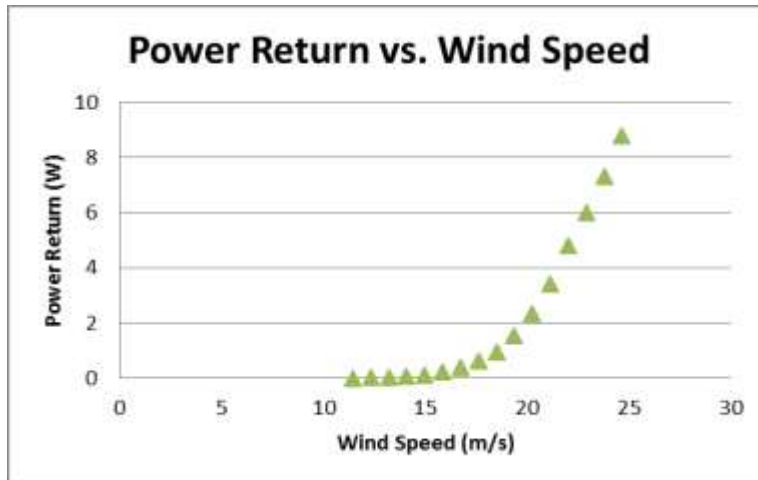


Figure 2: Power return as a function of wind speed

When we ran the Matlab script for various descent angles, we found that steeper descent angles produced a higher terminal and average velocity but took shorter time to complete the descent (see appendix 2). We observed that descent angles from -5 to -60 degrees failed to exceed the minimal wind speed required to spin the propeller and would therefore not produce any power. These descent angles were discarded. For the angles that would produce power (-65 to -85), we determined the energy return and the energy return rate using the procedure described in our methods. Our data is tabled and plotted below:

Descent Angle	Average Energy Regeneration Rate During Descent (W)	Total Energy Recovered (J)
-65	0.0450	1.778
-70	0.0842	2.891
-75	0.168	4.925
-80	0.836	21.41
-85	7.37	160.0

Table 1: Regenerative Braking Results

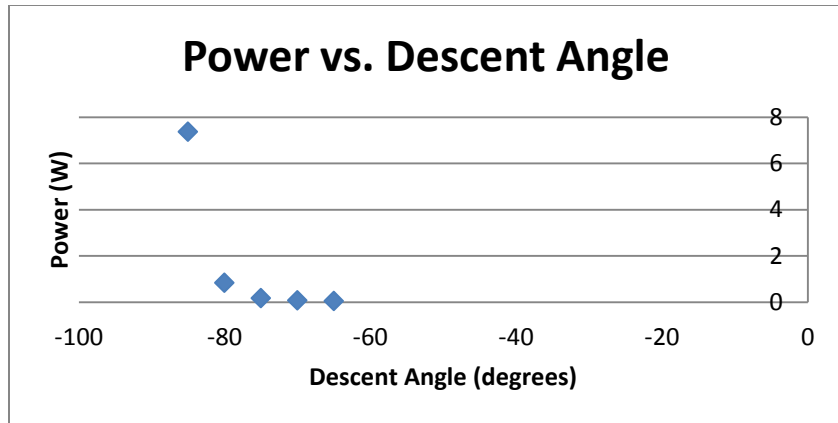


Figure 3: Energy rate (power) return

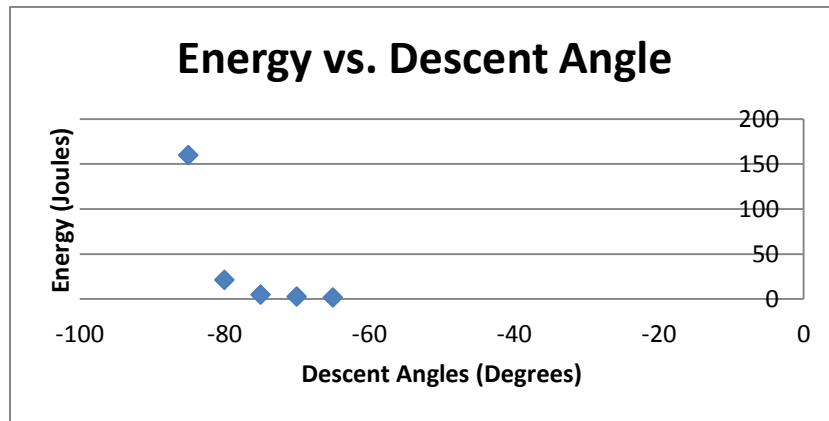


Figure 4: Energy return

From this data we concluded that even though -85 had the shortest descent time, it produced the largest energy return and return rate. Because the relationship between air speed vs. power produced was so aggressive; increasing faster than an exponential function, the higher winds speed produced a significantly higher power even over a much shorter time.

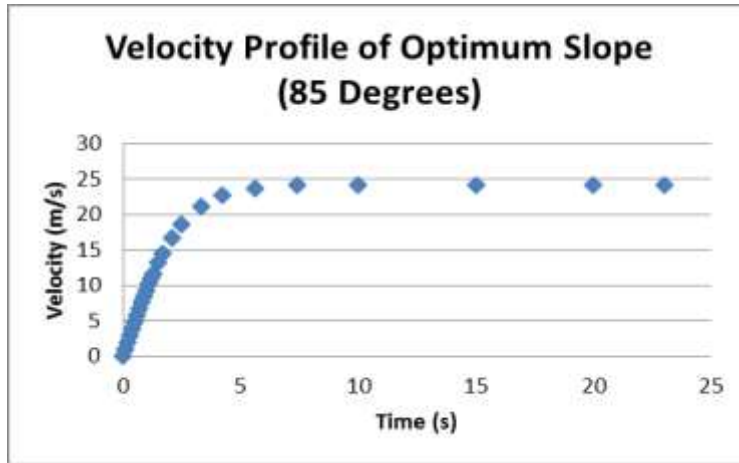


Figure 5: Velocity profile of optimum slope

The model RC aircraft uses an average of 20 Watts during flight. A descent angle of -85 degrees produces an average of 7 Watts over the course of the descent- roughly one third of our power consumed. Assuming zero energy required to obtain a height high enough to begin descent by riding a thermal, the aircraft would gain 1 minute of flight time per 2 minutes 52 seconds spent in a descent at an angle of -85 degrees. Because of the comparatively short energy return, this does not appear to be a practical solution to increasing the energy of the batteries to increase flight duration. However, the goal of our experiment was to prove the concept of regenerative braking in MAVs. We have determined that it is possible to regenerate energy during an aircraft's descent and that the energy return rate is of the same order of magnitude as energy consumption. Additional work should be conducted to improve the energy return rates possible during descent to improve practicality.

Data Limitations

We had to overcome limitations dictated by available hardware. We were limited to using the constant gear ratio motor that was provided with the RC aircraft. A variable gear ratio (transmission) could significantly improve the power return because the minimum propeller spin speed (MPSS) was caused by friction and resistance within our motor. If the resistance of the motor could be mitigated by manipulating the gear ratio, the MPSS could be reduced and a greater variety of descent angles could

overcome the MPSS. This would generate a greater number of candidates for the optimal recharge descent angle.

The second limitation was the inability to use a battery recharging unit as the primary load in our circuit when testing for power. Instead, we estimated the resistance of a Nickel Cadmium battery during recharging by using battery specifications. We placed a comparable resistor in the circuit to simulate the charging battery. While it does yield a reasonable estimate, future tests should use a recharging circuit.

Some limitations were self-imposed for simplicity. We built our Matlab script to only consider constant descent angles during recharge flight. We did this to limit the scope and complexity of the problem. Future work would benefit from the inclusion of a greater variety of descent paths. Other limitations of our Matlab script include the simplification of air density. We considered air density constant; however, it does vary with altitude, temperature, and location and should be a factor in future optimizations.

Our testing results and analysis showed that using inertial recovery to regenerate the battery in flight is possible, but not currently practical. The energy returns we calculated from the descent were lower than the energy consumption rate and the aircraft would need to spend more time in a recharge descent than engaged in a mission. We recommend further research that addresses previously mentioned limitations and explores methods of producing more energy during descent (such as increasing the terminal velocity). Lastly, research should be done on thermal tracking to make it efficient for the MAV mission. If MAVs can harness this energy over a target area quickly, it could produce a substantial increase in energy for the batteries. This would increase the flight duration and would make the inertial recovery system practical.

Laser method

The goal of our experiment was to demonstrate the overall feasibility of a laser transfer system by completing a small scale proof of concept. The experiment for this proof of concept was run as described in the methods. For each of our three tests, solar output power varied by less than 8% and the temperature varied by less than 5% for each power level. On the below figure, the X-axis displays the actual optical output of the laser as measured by a photo detector. This is the actual power striking the solar cell for each measurement, measured in mW. The left Y-axis and blue plot line display the power outputted by the solar cell from the laser transmission divided by the laser dot size area. The right Y-axis and red plot line display the temperature at the surface of the solar cell at the end of the 30 second transmission period for each power level. Below, the average values for the two experiment trials were plotted. The data for graph can be seen in appendix 3.

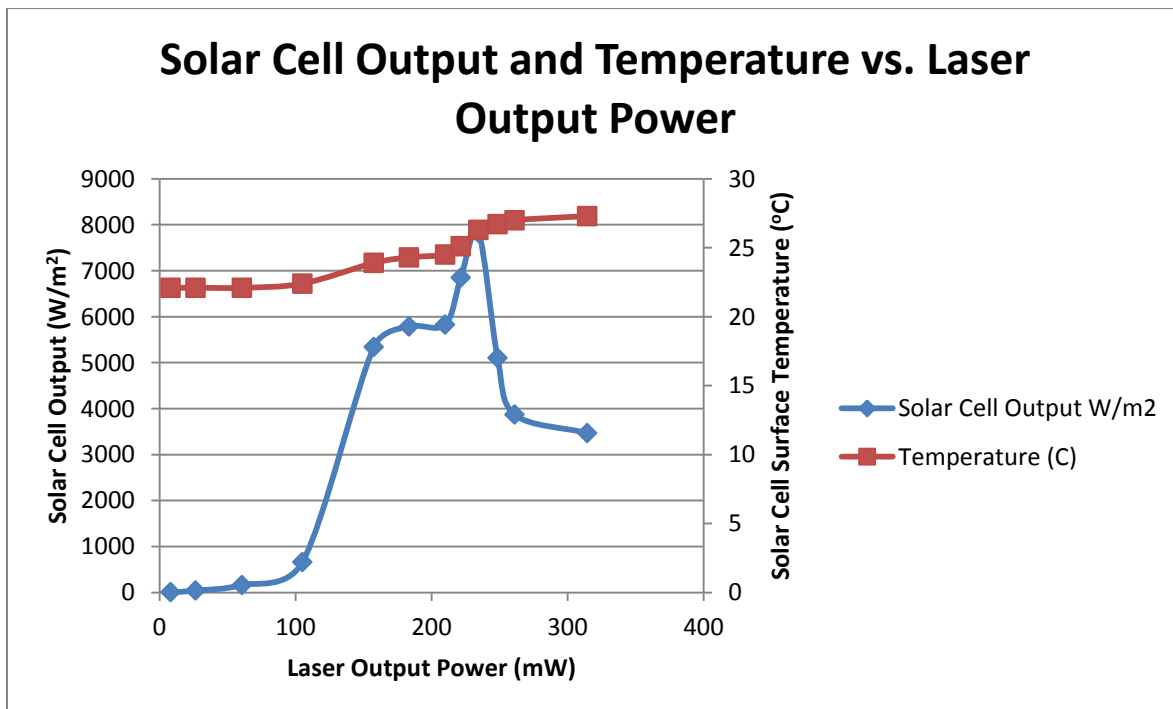


Figure 6: Plot of results of laser experiment

In the above figure, the solar output power initially increases as the power output from the laser increases. However, the maximum power transfer rate occurs when the laser output power is 235 mW and the solar cell output per laser area is 7825 W/m². After this point the power return from the solar cell decreases. This is likely due to the decrease in performance at elevated temperature. As the temperature increases at the surface of the solar cell with the laser output, the solar cell conversion efficiency decreases. When the solar cell exceeds a temperature of 26.3 °C, the conversion efficiency significantly decreased. There is a conversion efficiency “sweet spot” which occurs between 5340 W/m² and 7825 W/m². During this range the efficiency is at its highest; approximately .07% as shown in the graph below.

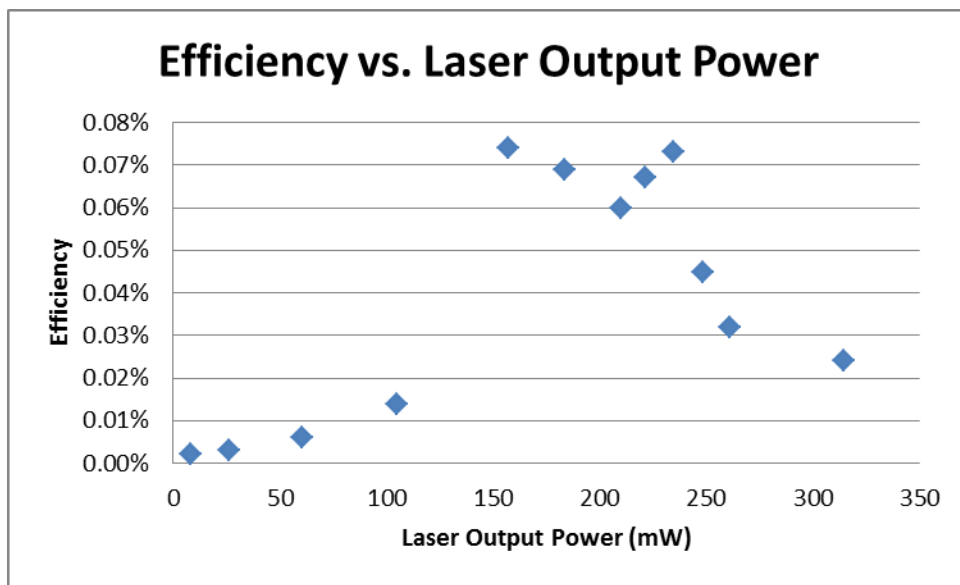


Figure 7: Solar Cell Efficiency

The efficiency value we found is relatively low when compared to our initial testing results. Our control test for our solar cell showed that it was operating at only 5.1% efficiency. In recent lab tests, the Panasonic Corporation achieved a conversion efficiency of 25.6%; significantly more efficient than our solar cell (Davis, 2014). This low conversion efficiency value can be explained by solar cell wavelength mismatch and poor quality solar cell. Solar cells are optimized for converting energy from the sun (peak

wavelength 500nm). Due to equipment availability, the laser we used had a wavelength of 994 nm; well outside the normal operating range of solar cells. Most of the energy from the laser passed through the solar cell or reflected off the solar cell because the cell is not optimized for such a high wavelength. The additional reason for poor conversion efficiency was because the solar cells we tested with were of low quality.

Application to aircraft

We recognize that for the real-world application of a laser to solar cell energy transfer system, a different laser and solar cell are required. The solar cell should be of significantly higher efficiency. Additionally, the laser wavelength needs to better match the efficiency curve of the solar cell; this will produce a more efficient energy transfer. Finally, the laser should be of significantly higher power. In order to maximize the efficiency of the energy transfer, the more powerful laser beam should be expanded to strike a larger area than the laser beam we experimented with during our project. By experimentally determining the optimal power per area of our transfer, we can determine the area that the more powerful laser beam must strike. We propose increasing the power and area struck by the same factor to maintain the optimal power transferred per area of solar cell.

As previously discussed, we experimentally determined that our solar cell could transfer a maximum of 7825 W/m^2 . The watts unit refers to energy produced by the solar cell and the m^2 is area of the solar cell. In order for a solar cell to produce 60 W (3 times the power consumption of our RC aircraft), the transfer laser should strike 76 cm^2 of solar cell to maintain the optimal 7825 W/m^2 . This would avoid damaging the solar cell as in the solar kite experiment mentioned in our background. Assuming that the laser's wavelength is optimized for the solar cell, and a 20% conversion efficiency, a laser power of 300 W is required to output 60 W.

Configuring a 300 W laser to strike 76 cm² of solar cell is a challenging obstacle. A method of tracking the aircraft is required so that the laser reliably strikes the proper location on the aircraft. As the distance between the aircraft and the laser would constantly change during flight, a technique of appropriately expanding the beam is required. There are two ways beam expansion is achievable, first is to use a variable magnification beam expander at the laser source. In this method, the tracking system could determine the distance between the laser and aircraft and adjust the magnification to strike the proper area on the aircraft. The benefit of this is minimal added weight on the aircraft (most of the added weight is on the ground). In the second method of achieving beam expansion, the expansion lens has a constant magnification and is located on the aircraft. It is simpler but places additional weight on the aircraft. Additional research is required to determine which method is best suited for aircraft energy transfer applications. Both methods are depicted below:

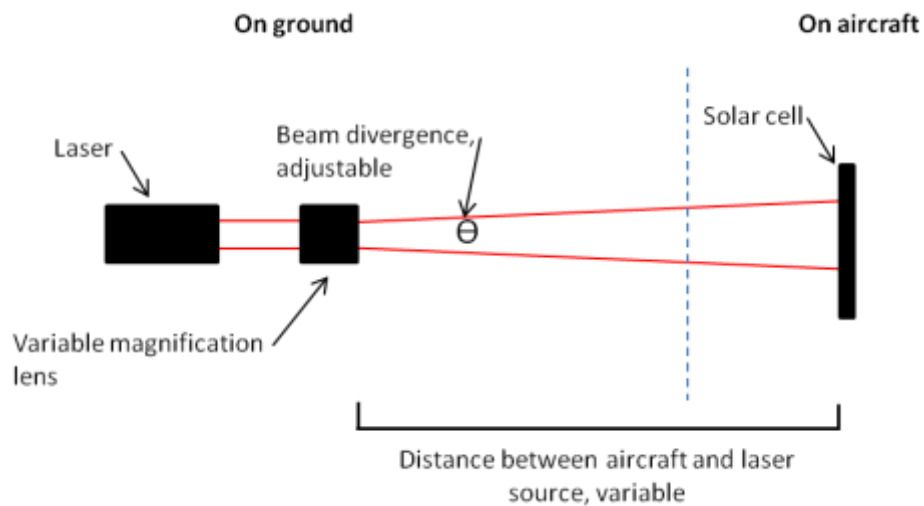


Figure 8: Method 1, Variable Magnification Lens on Ground

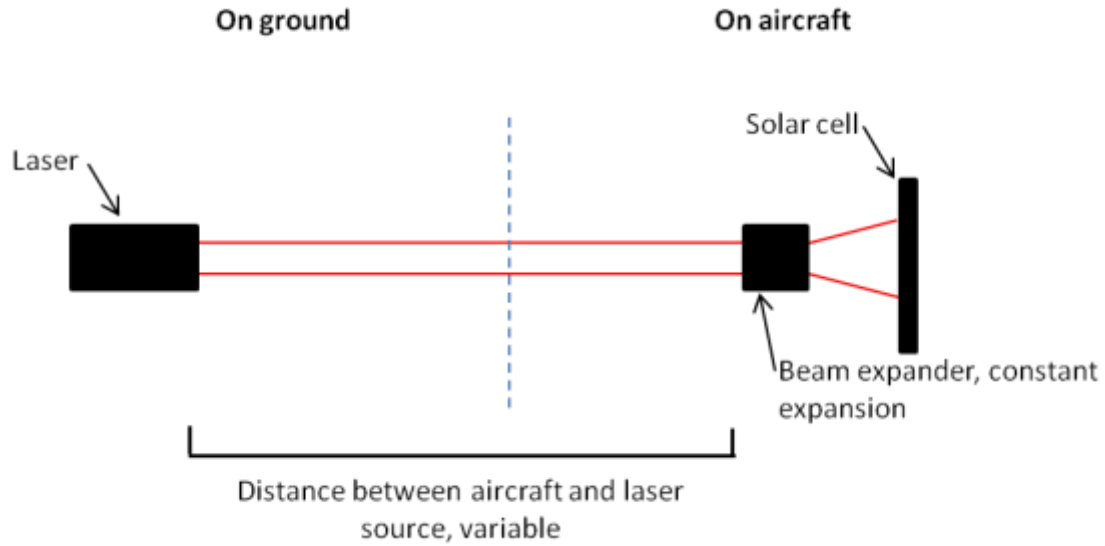


Figure 9: Method 2, Constant Magnification Lens on Aircraft

We determined that the laser energy transfer system is potentially feasible. However, more research is required to determine efficiency and performance when the wavelength of the laser is optimized for the solar cell. Additionally, we assumed we could increase laser power as long as we proportionally increased the area to keep the optimal transfer per area of 7825 W/m^2 that was determined by our experiment. Lastly, testing with high powered lasers needs to be conducted to confirm this assumption, and a tracking system must be created that can operate efficiently and reliably.

Conclusion

Our project sought to obtain proof of concept of two methods of recharging a MAV in flight. The first method we examined was the inertial recovery system. Our testing demonstrated that while possible, it is not a practical method of extending flight duration and more research is required. The return of 7 W, or approximately one-third of average power consumption for our RC model, was not high enough to significantly increase flight time. Our second method, the in-flight laser transmission, showed more promise if scaled appropriately. With the correct equipment and additional research, our testing demonstrates the strong potential to transfer enough energy to significantly impact the flight duration of a MAV. Our goal of proof of concept was achieved for both methods and the window for more research and advancement opened.

Bibliography

AeroVironment News & Events (2013, August 12). *AeroVironment Solar-Powered Puma AE Small Unmanned Aircraft Achieves Continuous Flight for More Than Nine Hours*. Retrieved from http://www.avinc.com/resources/press_release/aerovironment-solar-powered-puma-ae-small-unmanned-aircraft-achieves-contin

AeroVironment Puma Data Sheet (2013, November 19). *Puma AE Data Sheet*. Retrieved from http://www.avinc.com/uas/small_uas/puma/

AeroVironment Raven (2013). *UAS: RQ-11B Raven*. Retrieved from http://www.avinc.com/downloads/Raven_Gimbal.pdf

Alta Devices Technology (2013). *Mobile Power Technology*. Retrieved from <http://www.altadevices.com/technology-overview.php>

Davis, S. (2014, April 14). *Solar Cell Achieves 25.6% Energy Conversion Efficiency In Lab*. Retrieved from <http://powerelectronics.com/blog/solar-cell-achieves-256-energy-conversion-efficiency-lab>

Edwards, D., Silberberg, L. (2010, September). *Autonomous Soaring: The Montague Cross-Country Challenge*. Retrieved from <http://arc.aiaa.org/doi/pdf/10.2514/1.C000287>

Kawashima, N., Kazuya, T. (2008). *Laser Energy Transmission for a Wireless Energy Supply to Robots*. Retrieved from http://cdn.intechopen.com/pdfs/5576/InTech-Laser_energy_transmission_for_a_wireless_energy_supply_to_robots.pdf

Matsumoto, H. (2002, December). *Research on Solar Power Satellites and Microwave Power Transmission in Japan*. Retrieved from <http://ieeexplore.ieee.org/xpl/articleDetails.jsp?reload=true&arnumber=1145674&contentType=Journals+%26+Magazines>

NASA: Lasers. (2013). *What is a laser?* Retrieved from <http://spaceplace.nasa.gov/laser/en/>

San Jose State University. (2014). *Solar Photovoltaic (PV) Cells*. Retrieved from <http://www.engr.sjsu.edu/trhsu/Chapter%2020on%20solar%20PV%20%5BCompatibility%20Mode%5D.pdf>

Scott, J. (2005, December 4). *Birds, Thermals & Soaring Flight*. Retrieved from <http://www.aerospaceweb.org/question/nature/q0253.shtml>

(Soarfl) Seminole-Lake Gliderport Soaring Site (2013). *How Gliders Fly*. Retrieved from http://soarfl.com/How_Gliders_Fly.html

Solar Impulse HB-SIA Datasheet (2013). *Solar Impulse HB-SIA*. Retrieved from <http://www.solarimpulse.com/en/airplane/hb-sia/>

Sukhatme, S. P., Nayak J.K. (2008). *Solar Energy, Principles of Thermal Collection and Storage*. New Delhi: Tata McGraw-Hill.

Summerer, L., Purcell O. (2009). *Concepts for Wireless Energy Transmission Via Laser*. Retrieved from <http://www.esa.int/gsp/ACT/doc/POW/ACT-RPR-NRG-2009-SPS-ICSOS-concepts-for-laser-WPT.pdf>

Tech Bulletin. (1994). *Nickel-Cadmium and Lead-Acid Battery Comparisons*. Retrieved from http://www.isco.com/webproductfiles/applications/201/nicad_vs_leadacidbatteries_techbulletin.pdf

Turpen, A. (2013). *How Regenerative Braking Works*. Retrieved from <http://www.futurecars.com/technology/how-regenerative-braking-works>

Appendix 1: Wind Tunnel Testing Data

This appendix has the data from the three tests that we ran in the wind tunnel to determine how much power the motor produced at certain wind speeds.

Test 1

MPH	m/s	Hz	Volts	Resistance	Power (W)
55.11809	24.63999	28	3.27	1.2	8.9
53.14959	23.75999	27	2.90	1.2	7
51.18109	22.87999	26	2.71	1.2	6.1
49.21258	21.99999	25	2.47	1.2	5.1
47.24408	21.11999	24	2.08	1.2	3.6
45.27558	20.23999	23	1.73	1.2	2.5
43.30707	19.35999	22	1.40	1.2	1.6
41.33857	18.47999	21	1.07	1.2	0.95
39.37007	17.59999	20	0.81	1.2	0.55
37.40156	16.71999	19	0.64	1.2	0.34
35.43306	15.83999	18	0.46	1.2	0.18
33.46456	14.96	17	0.33	1.2	0.09
31.49605	14.08	16	0.22	1.2	0.04
29.52755	13.2	15	0.05	1.2	0.0021
27.55905	12.32	14	0.03	1.2	0.0009
25.59054	11.44	13		1.2	0
23.62204	10.56	12		1.2	0
21.65354	9.679997	11		1.2	0
19.68503	8.799997	10		1.2	0
17.71653	7.919997	9		1.2	0
15.74803	7.039998	8		1.2	0
13.77952	6.159998	7		1.2	0
11.81102	5.279998	6		1.2	0
9.842517	4.399999	5		1.2	0
7.874013	3.519999	4		1.2	0
5.90551	2.639999	3		1.2	0
3.937007	1.759999	2		1.2	0
1.968503	0.88	1		1.2	0

Test 2

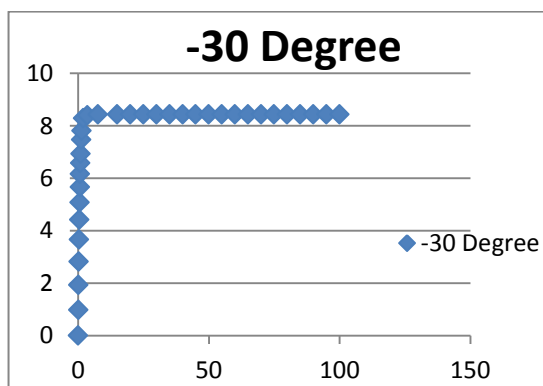
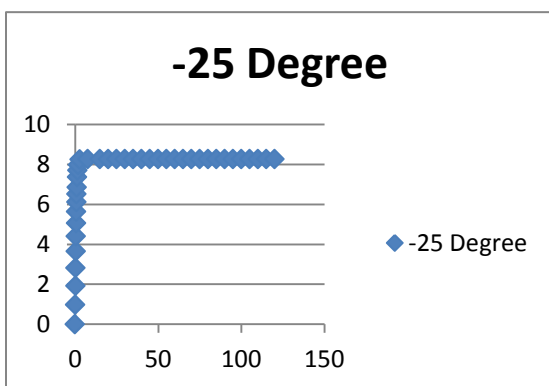
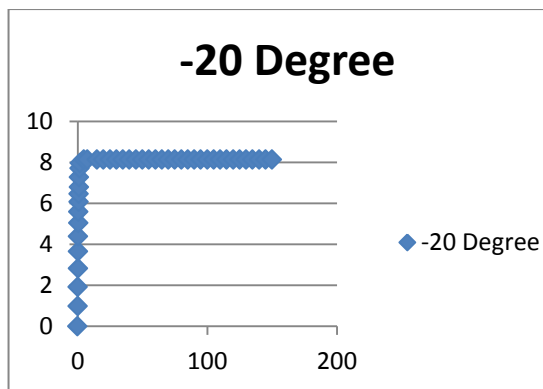
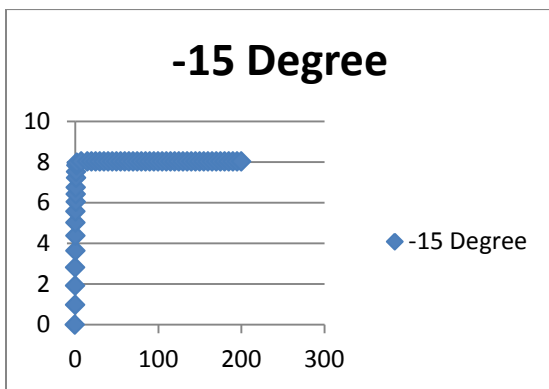
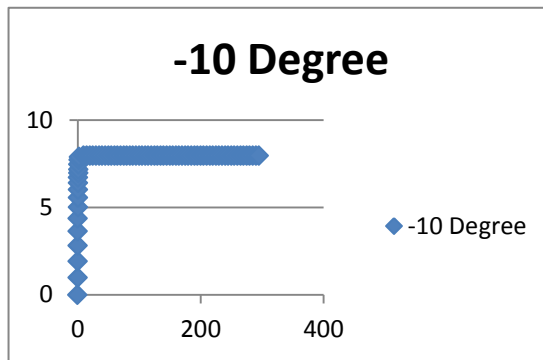
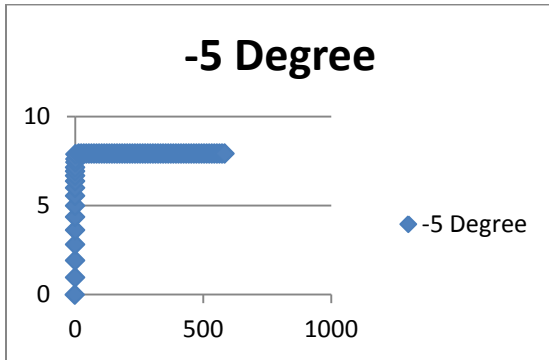
MPH	m/s	Hz	Volts	Resistance	Power (W)
55.11809	24.63999	28	3.23	1.2	8.7
53.14959	23.75999	27	3.00	1.2	7.5
51.18109	22.87999	26	2.73	1.2	6.2
49.21258	21.99999	25	2.45	1.2	5
47.24408	21.11999	24	2.08	1.2	3.6
45.27558	20.23999	23	1.73	1.2	2.5
43.30707	19.35999	22	1.33	1.2	1.5
41.33857	18.47999	21	1.04	1.2	0.9
39.37007	17.59999	20	0.89	1.2	0.7
37.40156	16.71999	19	0.72	1.2	0.4
35.43306	15.83999	18	0.53	1.2	0.2
33.46456	14.96	17	0.33	1.2	0.09
31.49605	14.08	16	0.29	1.2	0.07
29.52755	13.2	15	0.20	1.2	0.03
27.55905	12.32	14	0.15	1.2	0.020
25.59054	11.44	13	0.004	1.2	0.000
23.62204	10.56	12		1.2	0
21.65354	9.679997	11		1.2	0
19.68503	8.799997	10		1.2	0
17.71653	7.919997	9		1.2	0
15.74803	7.039998	8		1.2	0
13.77952	6.159998	7		1.2	0
11.81102	5.279998	6		1.2	0
9.842517	4.399999	5		1.2	0
7.874013	3.519999	4		1.2	0
5.90551	2.639999	3		1.2	0
3.937007	1.759999	2		1.2	0
1.968503	0.88	1		1.2	0

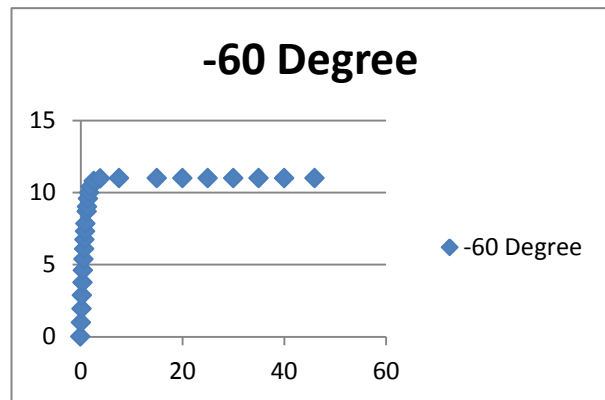
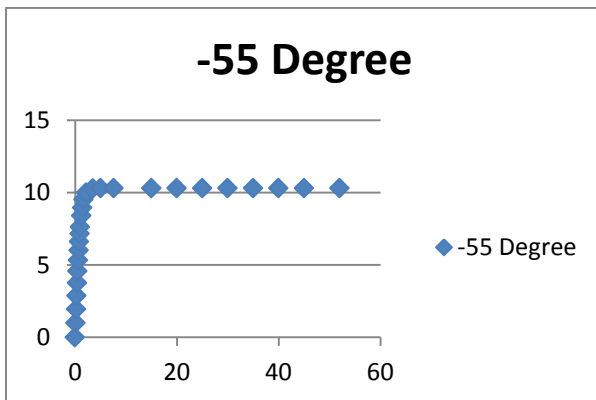
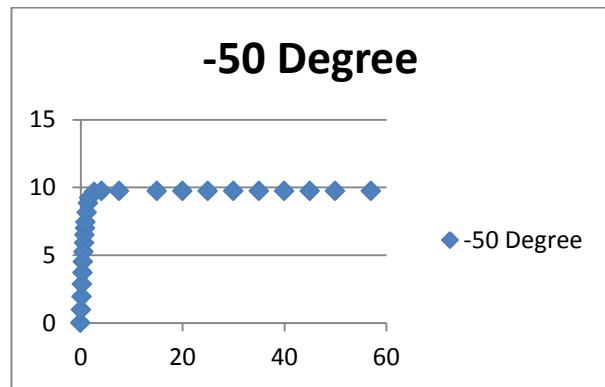
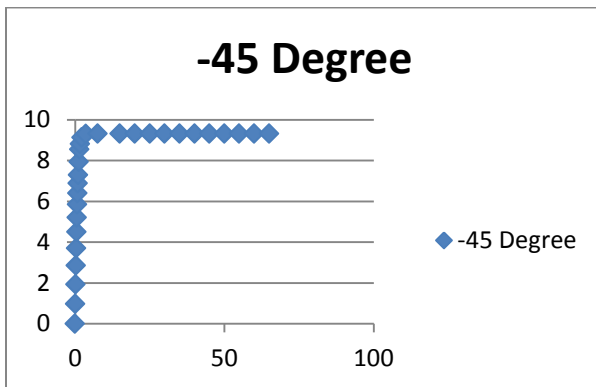
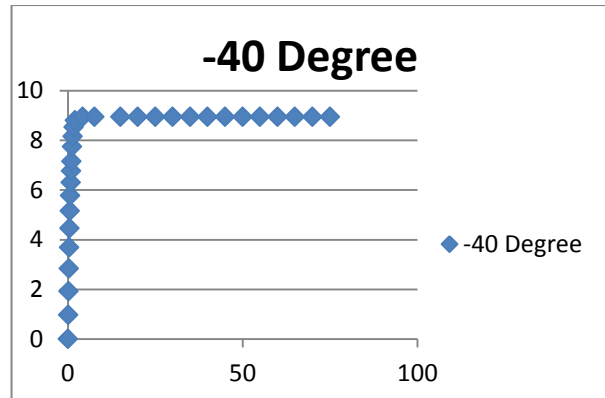
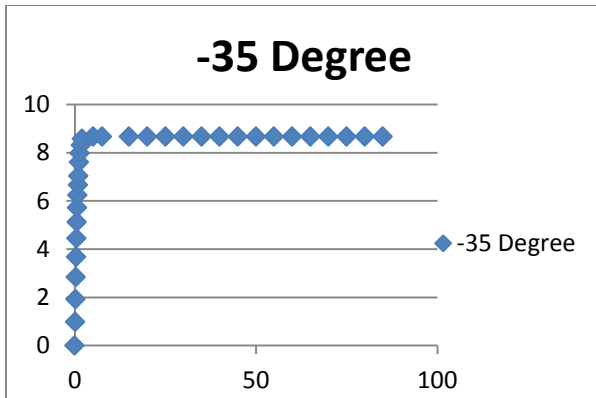
Test 3

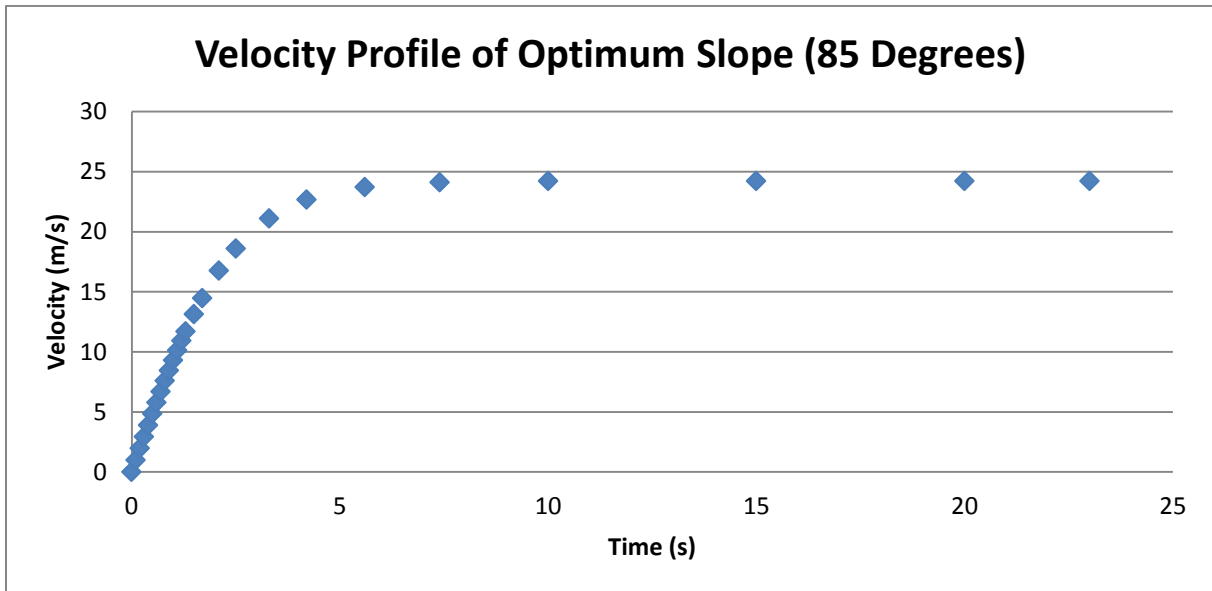
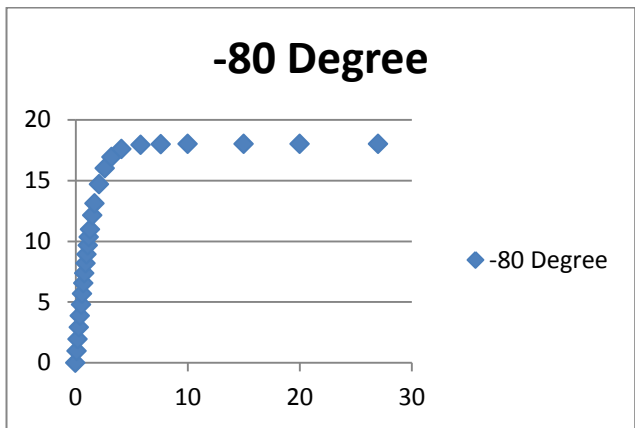
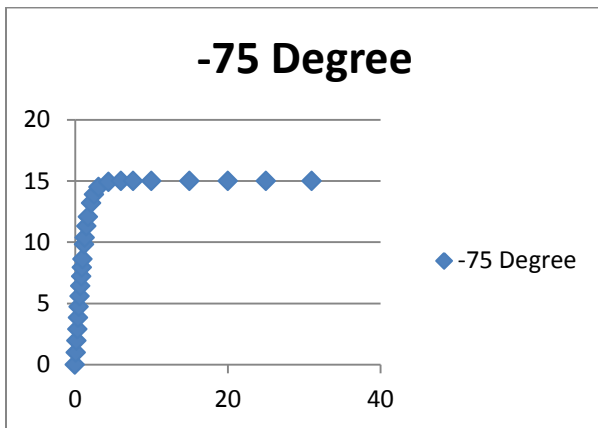
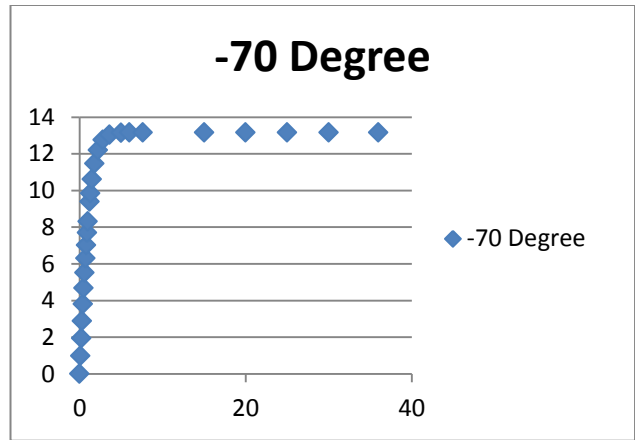
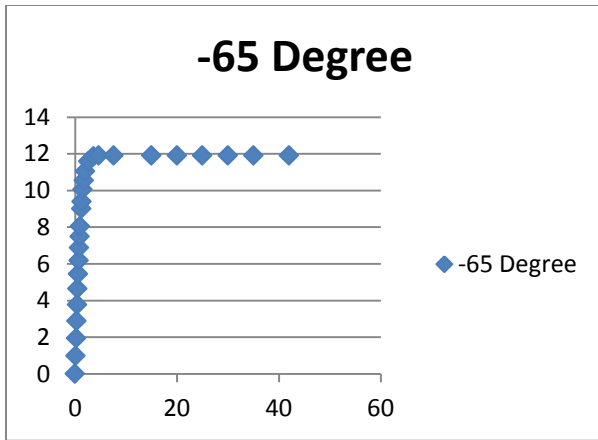
MPH	m/s	Hz	Volts	Resistance	Power (W)
55.11809	24.63999	28	3.25	1.2	8.8
53.14959	23.75999	27	2.96	1.2	7.3
51.18109	22.87999	26	2.68	1.2	6
49.21258	21.99999	25	2.40	1.2	4.8
47.24408	21.11999	24	2.02	1.2	3.4
45.27558	20.23999	23	1.68	1.2	2.35
43.30707	19.35999	22	1.39	1.2	1.3
41.33857	18.47999	21	1.06	1.2	1.13
39.37007	17.59999	20	0.85	1.2	1.02
37.40156	16.71999	19	0.68	1.2	0.94
35.43306	15.83999	18	0.50	1.2	0.85
33.46456	14.96	17	0.33	1.2	0.76
31.49605	14.08	16	0.27	1.2	0.73
29.52755	13.2	15	0.15	1.2	0.68
27.55905	12.32	14	0.11	1.2	0.65
25.59054	11.44	13		1.2	1E+00
23.62204	10.56	12		1.2	0
21.65354	9.679997	11		1.2	0
19.68503	8.799997	10		1.2	0
17.71653	7.919997	9		1.2	0
15.74803	7.039998	8		1.2	0
13.77952	6.159998	7		1.2	0
11.81102	5.279998	6		1.2	0
9.842517	4.399999	5		1.2	0
7.874013	3.519999	4		1.2	0
5.90551	2.639999	3		1.2	0
3.937007	1.759999	2		1.2	0
1.968503	0.88	1		1.2	0

Appendix 2: Descent Profiles for Different Constant Descent Angles

This appendix has the graphs that plot the Matlab data for descent angles -5 through -85. The speed is in m/s is on the y-axis and the time in seconds is on the x-axis.







Appendix 3: Average Data from Laser Tests

This appendix contains the laser output power and the resulting solar cell output power, temperature at the surface at the end of 20 seconds, conversion efficiency, and solar cell output power per bombarded area of solar cell.

Laser output power (mW)	Solar cell output power (mW)	Temperature (°C)	Efficiency	Solar cell output per solar cell area (W/m ²)
8	0.000	22.1	0.002%	6.861
26.5	0.001	22.1	0.003%	40.22
60.5	0.004	22.1	0.006%	164.0
105	0.014	22.4	0.014%	663.2
157.5	0.116	23.9	0.074%	5340
183.5	0.126	24.3	0.069%	5786
210	0.127	24.5	0.060%	5828
221.5	0.149	25.1	0.067%	6853
234.5	0.170	26.3	0.073%	7825
248.5	0.111	26.7	0.045%	5101
261	0.084	27.0	0.032%	3872
314.5	0.075	27.4	0.024%	3469